J Fluoresc (2010) 20:269–274
DOI 10.1007/s10895-009-0550-3

ORIGINAL PAPER

A Fiber-Optic Evanescent Wave O_2 Sensor Based on Ru(II)-Doped Fluorinated ORMOSILs

Yan Xiong · Daoqian Zhu · Shiheng Chen · Hong Peng · Yafeng Guan

Received: 10 June 2009 / Accepted: 28 September 2009 / Published online: 13 October 2009

Abstract A novel fiber-optic evanescent wave sensor (FOEWS) for O_2 detection based on $[Ru(bpy)_3]^{2+}$-doped hybrid fluorinated ORMOSILs (organically modified silicates) has been developed. The sensing element was fabricated by dip-coating the optical fiber with $[Ru(bpy)_3]^{2+}$-doped hybrid fluorinated ORMOSILs composed of *n*-propyltrimethoxysilane (*n*-propyl-TriMOS) and 3, 3, 3-trifluoropropyltrimethoxysilane (TFP–TriMOS). Fluorophores of $[Ru(bpy)_3]^{2+}$ were excited by the evanescent wave field produced on the fiber core surface and the emission fluorescence was quenched by O_2. Spectroscopic properties have been characterized by FTIR and UV–VIS absorption measurements. By using the presented hybrid fluorinated ORMOSILs, which enhances the coating surface hydrophobicity, the quenching response is increased. The sensitivity of the sensor is 7.5, which is quantified in terms of the ratio I_{N2}/I_{O2} (I_{N2} and I_{O2} represent the fluorescence intensities in pure N_2 and pure O_2 environments, respectively). The limit of detection (L.O.D.) is 0.01% (3σ) and the response time is about 1 s. Meanwhile, the proposed FOEWS has the advantages of easy fabrication, low cost, fast response and suitable sensitivity for oxygen monitoring using a cheap blue LED as light source and coupling a miniature PMT detector directly to the optical fiber probe.

Keywords Fiber-optic sensor · Evanescent wave · Hybrid fluorinated ORMOSILs · Oxygen detection

Y. Xiong · D. Zhu · S. Chen · H. Peng · Y. Guan (✉)
Department of Instrumentation and Analytical Chemistry,
Dalian Institute of Chemical Physics,
Chinese Academy of Sciences,
Dalian 116023, China
e-mail: guan_yafeng@yahoo.com.cn

Introduction

Oxygen (O_2) sensing is of major importance in many chemical and biological applications. The two most common methods employed for O_2 detection are Winkler titration approach and the Clark electrode. However, they either need long response time and complex operation procedure, or consume O_2 and are used mainly for sensing dissolved O_2. Optical O_2 sensors offer the advantages of not consuming O_2, having shorter response time and being used for measuring O_2 in both gas and aqueous phases. They are mainly based on the quenching of fluorescence or phosphorescence by molecular O_2 and are extensively applied in the chemical [1], clinical [2] and environmental fields [3].

During the optical O_2 sensor fabrication process, luminescent molecules are commonly immobilized in solid matrixes, which act as media for supporting the sensor dyes and for O_2 permeability from the surroundings [4]. Therefore, the sensor performance strongly depends on the immobilization method used to host the O_2-sensitive luminophores. Among developed immobilization methods, physisorption commonly suffers from sensing material leakage though the physisorption process is very simple; covalent attachment can eliminate the leaching problem at the cost of complex chemistry reaction, time-consuming and high cost. As a result, sequestration of the recognition chemistry within a porous, three-dimensional network has become an attractive mean to alleviate the above-mentioned immobilization problems. Sol-gel oxides (xerogels) with excellent chemical, photochemical and thermal stability were attractive for fluorophores immobilization. A significant number of optical O_2 sensors based on sol–gel-derived materials have been reported in the literature [5–13]. However, those inorganic sol–gel-based O_2 sensors commonly suffer from unstable response and nonlinear

Stern–Volmer plots together with shrinkage and pore collapse of sensing film along the time.

ORMOSILs (organically modified silicates), which can reduce the degree of cross-linking, improve film adhesion to its support, reduce the concentration of surface silanol groups and alter partition coefficients, have been developed to improve the sol–gel glasses performance [14, 15]. ORMOSILs using allows the preparation of tailor-made xerogels-based composites to possess typical properties of organic materials such as flexibility and mechanical strength as well as benefits of inorganic materials such as high tensile strength and chemical resistance. In recent years, new fluorinated ORMOSILs were developed [16, 17] and have been applied in several sensing applications [18–20].

The fiber-optic evanescent wave sensor (FOEWS), which avoids laborious optical adjustment, has been conveniently and effectively used in many practical applications [21–26]. The evanescent wave (EW) field is produced by total internal reflection (TIR, a fundamental characteristic of an optic fiber) and its intensity decays exponentially from the fiber core surface into the medium. The EW field can excite fluorophores immobilized on the core surface and the produced fluorescence is then coupled back into the fiber core to the detection system.

In this paper, we present the details of a simple, sensitive and low cost LED sourced fiber-optic evanescent wave O_2 sensor (FOEWS) based on novel hybrid fluorinated ORMOSILs coating. The sensing coating was fabricated by dip-coating the optical fiber with $[Ru(bpy)_3]^{2+}$-doped hybrid ORMOSILs that are composed of alkyl ORMOSIL *n*-propyltrimethoxysilane (*n*-propyl-TriMOS) and perfluoroalkyl ORMOSIL 3, 3, 3-trifluoropropyltrimethoxysilane (TFP–TriMOS). The fluorophores of $[Ru(bpy)_3]^{2+}$ were immobilized into the ORMOSILs-based coating and were excited by the evanescent wave field. Emission fluorescence was quenched by the presence of oxygen and quenching response is increased with the enhancement of the coating surface hydrophobicity by using the presented hybrid fluorinated ORMOSILs. UV and FTIR have been used to study the spectroscopic properties and the performances of the presented FOEWS for O_2 detection are reported in detail.

Experimental section

Reagents and materials

$[Ru(bpy)_3]^{2+}$ was purchased from Fluka (USA). TFP–TriMOS and *n*-propyl-TriMOS were kindly supplied by Feidian Trade Ltd. (Hangzhou, China) and Nengde Chemical Co., Ltd. (Nanjing, China), respectively. HCl and EtOH were obtained from Shenyang Chemical Reagent Company (Shenyang, China). All reagents were of analytical grade and used as received.

Apparatus and optical systems

Figure 1 illustrates the experimental setup system for O_2 sensing. The plastic coated silica (PCS) optical fiber (core diameter = 400 μm, NA = 0.37) was purchased from Chunhui Inc., Ltd. (Nanjing, China). A blue lamp LED (Shifeng Co. Ltd., Shenzhen, China) was used as the excitation light source. A photomultiplier (PMT R928, Hamamatsu, Japan) was used for the fluorescence signal detection that passed through a long-pass filter (LP 610 nm; Bodian Optical Corp. Ltd., Beijing, China). The UV–Vis lambda 35 spectrometer (Perkin Elmer, USA) and the spectrum 100 FTIR spectrometer (Perkin Elmer, USA) were used to detect the UV and FTIR absorbance, respectively. Different O_2 concentrations were obtained by mixing O_2 and N_2 and controlled through gas flowmeters.

Preparation of optical fiber probe

Adopting a similar approach to that used by Bukowski et al. [16], a composite precursor solution was prepared by mixing TFP-TriMOS (1.5 mL) and *n*-propyl-TriMOS (0.69 mL). Then EtOH (1.5 mL), deionized water (0.635 mL) and HCl (0.08 mL of 0.1M HCl) were added to the sol solution to catalyze the ORMOSIL reaction. The solution was then capped and sonicated for 1 h.

$[Ru(bpy)_3]^{2+}$ was dissolved in EtOH to form 5 mM sensor dye solution. The luminophore-doped sol solution was prepared by physically mixing 20 μL of 5 mM $[Ru(bpy)_3]^{2+}$ with 80-μL portion of the prepared TFP-TriMOS / *n*-propyl-TriMOS sol solution. This fluorinated xerogels-based mixture was sonicated under ambient conditions for 10 min prior to fiber coating.

A 20-cm long PCS optical fiber was used and a 6-cm region in the middle of the fiber was decladded by exposing it to a flame which burned the plastic clad. The decladded region was immersed in NaOH solution 0.1M for 24 h and

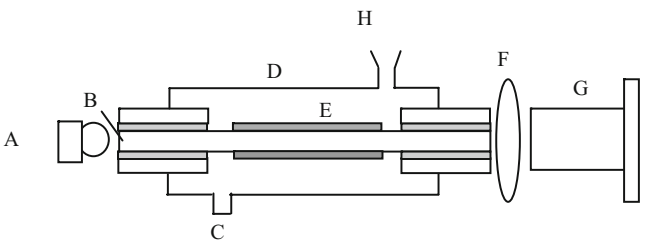

Fig. 1 Schematic diagram of fiber-optic O_2 sensor system by evanescent wave excitation: A, blue LED; B, optical fiber; C, gas inlet; D, flow cell; E, sensing coating doped with $[Ru(bpy)_3]^{2+}$; F, long-pass filter (LP610); G, photomultiplier (PMT); H, gas outlet

then washed in water and ethanol prior to coating. The decladded section of the fiber was then dip-coated by slow withdrawal from the coating solution. After coating, the fiber was dried for at least 72 h. Then the dried fiber was put into a homemade flow cell. The flow cell volume was about 0.4 mL and the gas flow rate was 150 mL/min. All of the procedures were performed at room temperature.

Results and discussion

Basic theory

Principle of Evanescent Wave (EW)

The sensor configuration employed by us relies on evanescent wave (EW) interactions between the guided radiation and an analyte-sensitive reagent. If total internal reflection (TIR) occurs, an evanescent wave (EW) field extends at the interface between the optically denser waveguide (refractive index n_1) and an optically thinner adjacent medium (refractive index n_2; with $n_1 > n_2$) [27]. The degree of penetration is often characterized by the penetration depth, d_p, which is the perpendicular distance from the interface at which the electric field amplitude, E, has fallen to $1/e$ of its value, E_0 at the interface [28] i.e.,

$$E = Eo \exp\left(-z/d_p\right) \tag{1}$$

The penetration depth, d_p, of the evanescent field is defined as [28]

$$d_p = \lambda \Big/ 2\pi\left(n_1{}^2 \sin^2\theta - n_2{}^2\right)^{1/2} \tag{2}$$

where λ is the wavelength of the radiation and θ is the incoupling angle. Absorbing species presented within the penetration depth of the evanescent field interact with radiation, resulting in attenuation of the frequencies where resonant energy transfer to the vibrational modes of molecules occurs.

Principle of fluorescence quenching sensing for O_2

If the luminescence quenching is purely dynamic, the excited–state lifetime and the intensity are related to the O_2 concentration. In the simplest situation of a luminophore in a homogeneous microenvironment, quenching takes place in accordance with the Stern–Volmer equations [4]:

$$I_0/I = \tau_0/\tau = 1 + K_{SV}[O_2] \tag{3}$$

$$K_{SV} = k_q \tau_0 = 4\pi g R N D \tag{4}$$

where I and τ are, respectively, the fluorescence intensity and excited-state lifetime of the luminophore, $[O_2]$ is the O_2 concentration, K_{SV} is the Stern–Volmer constant, k_q is the diffusion-dependent bimolecular quenching constant and the subscript 0 denotes the absence of O_2, g is the spin statistical factor, R is the collision radius, and N is Avogadro's number. It follows from Eqs. 3 and 4 that, for this ideal case, a plot of the I_0/I versus $[O_2]$ will be linear with an intercept at 1 and a slope of K_{SV}.

FEWS optical properties

Spectrum (A) in Fig. 2 (a) shows the absorption spectrum of the $[Ru(bpy)_3]^{2+}$-doped hybrid ORMOSILs used in the present O_2 sensor. As shown, the hybrid ORMOSILs has a Q band at 451 nm, corresponding to the deprotonated form of the sensor dye of $[Ru(bpy)_3]^{2+}$. The spectrum (B) in Fig. 2 (a) shows the emission spectrum of the blue LED light source measured by USB 4000 spectrometer. As shown, the center emission wavelength of the blue LED is

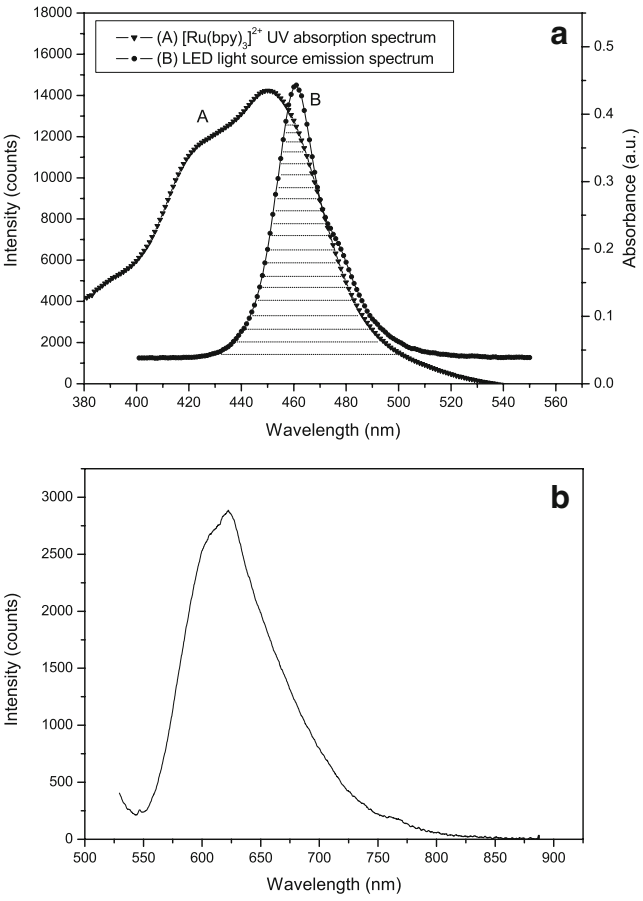

Fig. 2 **a** Spectrum A: absorption spectrum of $[Ru(bpy)_3]^{2+}$-doped xerogels. Spectrum B: LED emission spectrum. **b** Fluorescence emission spectrum of the $[Ru(bpy)_3]^{2+}$-doped sensors at room temperature

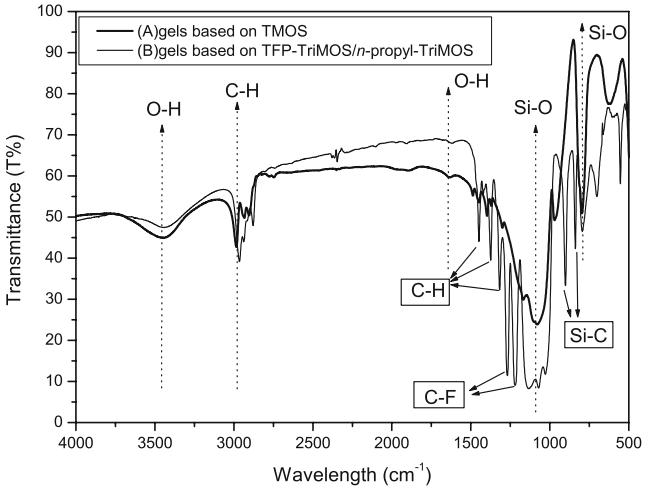

Fig. 3 FTIR spectra of dried gels of SiO_2: (A) based on pure TMOS and (B) based on TFP-TriMOS/*n*-propyl-TriMOS

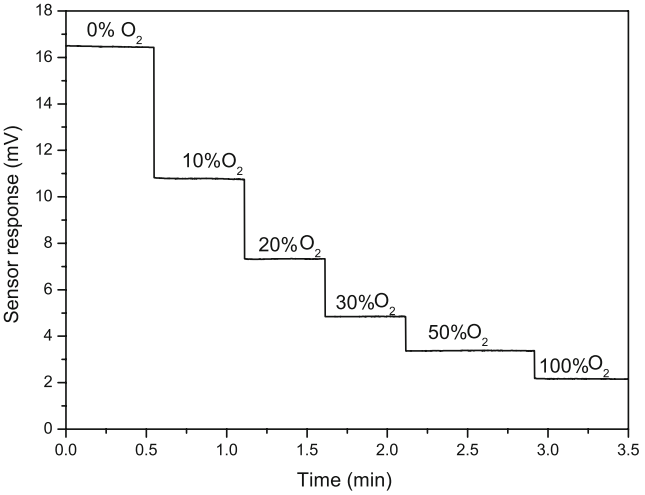

Fig. 5 Sensor response to varying oxygen concentrations of 0%, 10%, 20%, 30%, 50% and 100%

λ=462 nm, which is well–overlapped with the absorption spectrum of $[Ru(bpy)_3]^{2+}$ at the Q band. Illumination with the chosen LED results in fluorescence emission of the $[Ru(bpy)_3]^{2+}$-doped sensor at 622 nm which is presented in Fig. 2 (b). These results confirm the choice of the blue LED as the excitation light source for proposed FOEWS system.

Structure characteristics of the hybrid ORMOSILs by FTIR investigation

The structure characteristics of the presented hybrid fluorinated ORMOSILs-based materials have been investigated by Fourier Transform Infrared Spectroscopy (FTIR) and the spectra were analyzed in detail [29, 30]. Figure 3 presents the FTIR spectra of the dried gels based on (A) pure

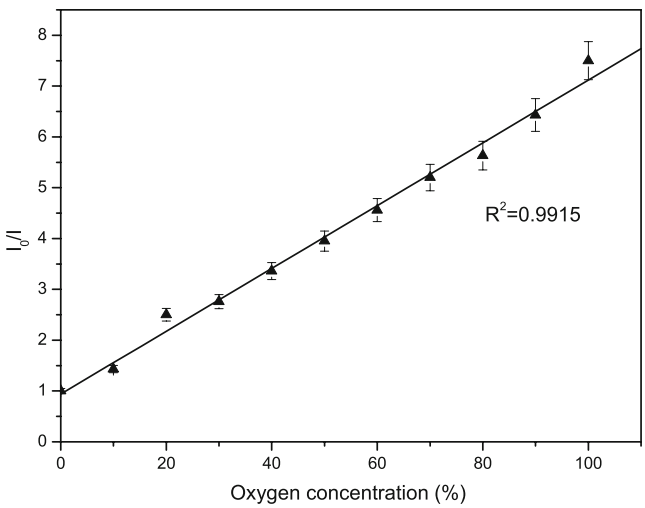

Fig. 4 Stern-Volmer plot of presented FOEWS based on TFP-TriMOS/*n*-propyl-TriMOS for oxygen detection

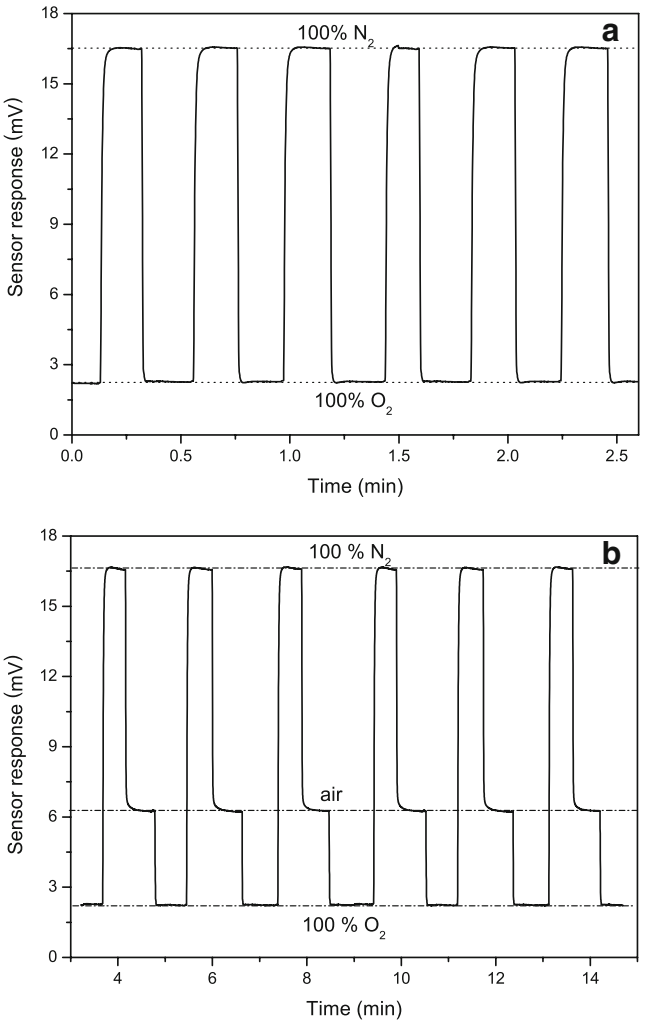

Fig. 6 **a** Typical dynamic response of the FOEWS switching between pure N_2 and pure O_2. **b** typical dynamic response of the FOEWS switching between pure N_2, air and pure O_2

TMOS and (B) TFP-TriMOS/ *n*-propyl-TriMOS, respectively. Both (A) and (B) show strong peaks at (1) 3,442 cm^{-1} corresponding to physical absorption of water; (2) around 2,980 cm^{-1} corresponding to stretching vibration of C–H bond; (3) 1,635 cm^{-1} corresponding to surface hydroxyl of Si–OH; (4) 1,071 cm^{-1} and 794 cm^{-1} corresponding to asymmetric and symmetric stretching vibration of Si–O–Si bond, respectively. For spectrum (B), it shows several other groups of strong peaks: (1) 1,449, 1,374 and 1,318 cm^{-1} corresponding to rocking vibration, wagging vibration and twisting vibration of C–H for CH_2, respectively; (2) at 1,269 cm^{-1} and 1,220 cm^{-1} corresponding to asymmetric and symmetric stretching vibration of C–F bond, respectively; (3) at 901 cm^{-1} and 838 cm^{-1} corresponding to vibration of Si–C bond, respectively. These above peaks do not exist in spectrum (A). In addition, the physical absorption peak of water at 3,442 cm^{-1} in spectrum (B) is much weaker than in spectrum (A). These differences between the two spectra indicate that the trifluoropropyl group ($CF_3CH_2CH_2$–) has been successfully modified onto the surface of the fluorinated xerogels material and the surface hydrophobicity of the fluorinated xerogels-based film has been improved significantly.

Sensor response behavior for O_2 detection

Sensitivity of the proposed O_2 FOEWS

The overall quenching response sensitivity in O_2 detection is given by I_{N2}/I_{O2}, where I_{N2} and I_{O2} represent the fluorescence intensities in pure N_2 and pure O_2, respectively. Figure 4 presents the Stern–Volmer plot for the presented $[Ru(bpy)_3]^{2+}$-doped TFP-TriMOS/*n*-propyl-TriMOS-based FOEWS in O_2 sensing. The Stern–Volmer plot provides an indication of the relative sensitivity of the $[Ru(bpy)_3]^{2+}$-doped sensor based on hybrid fluorinated ORMOSILs and the plot is linear to oxygen concentration in the range from 0 to 100%. From inspection, it is found that the sensitivity of the present FOEWS is 7.5 with R.S.D. = 2.1%. Figure 5 shows the response of the sensor to varying concentrations of O_2 and these data illustrate the repeatability, stability and high signal-to-noise ratio of the device. At the same time, the sensor exhibits highest sensitivity at lower concentrations of O_2.

Response time and Limit of Detection (LOD)

The parameter used to characterize response time in this study is the so-called t_{90} which is the time required for 90% change in the intensity reading of the equilibrium value. The response time is an important parameter in sensor design and characterization. For many applications, a short response time is desirable. Note that in acquiring the measurement results, the sampling frequency of the N2000 chromatographic data workstation was set to 20 ms in order to track the dynamic behavior of the sensor. Figure 6 (a) demonstrates the typical dynamic response of the FOEWS when switching between pure N_2 and pure O_2, and Fig. 6 (b) demonstrates the typical dynamic response of the FOEWS when switching between pure N_2, air and pure O_2. From inspection, it can be seen that t_{90} is 1.2 s when switching from O_2 to N_2 and 0.9 s when switching from N_2 to O_2. All of the plots show high values of signal-to-noise ratio with little evidence of photobleaching. The presented FOEWS yielded an LOD of 0.01% O_2.

Conclusions

In conclusion, a novel FOEWS for oxygen detection based on hybrid fluorinated ORMOSILs sensing coating immobilized with $[Ru(bpy)_3]^{2+}$ has been developed and characterized. By using *n*-propyl-TriMOS and TFP–TriMOS, the surface hydrophobicity of the sensing coating has been greatly improved and then the quenching performance of the FOEWS is remarkably increased. The sensor has a short response time of ~1 s and low L.O.D. of 0.01% for oxygen detection. Using a blue LED light source and a miniature PMT detection system, the presented FOEWS shows advantages of easy fabrication, low cost, fast response and suitable sensitivity for O_2 detection.

Acknowledgements This work was supported by the Chinese Academy of Sciences, Grant No. KZCX1-YW-14-3, and was partly supported by the Ministry of Science and Technology of China, Grant No.2008AA09Z110.

References

1. Demas JN, Degraff BA, Coleman PB (1999) Oxygen sensors based on luminescence quenching. Anal Chem 71:793A–800A
2. Tsukada K, Sakai S, Hase K, Minamitani H (2003) Development of catheter type optical oxygen sensor and applications to bioinstrumentation. Biosens Bioelectron 18:1439–1445
3. VanderDonckt E, Camerman B, Herne R, Vandeloise R (1996) Fiber-optic oxygen sensor based on luminescence quenching of a Pt(II) complex embedded in polymer matrices. Sens Actuators B: Chem 32:121–127
4. Lakowicz JR (1999) Principles of fluorescence spectroscopy, 2nd edn. Kluwer Academic/Plenum, New York
5. Xu H, Aylott JW, Kopelman R, Miller TJ (2001) M. A. Philbert, A real-time ratiometric method for the determination of molecular oxygen inside living cells using sol−gel-based spherical optical nanosensors with applications to rat C6 glioma. Anal Chem 73:4124–4133
6. Chan MA, Lam SK, Lo D (2002) Characterization of erythrosin B-doped sol-gel materials for oxygen sensing in aqueous solutions. J Fluoresc 12:327–332

7. McDonagh C, Kolle C, McEvoy AK, Dowling DL, Cafolla AA, Cullen SJ, MacCraith BD (2001) Phase fluorometric dissolved oxygen sensor. Sens Actuators B: Chem 74:124–130
8. Choi MMF, Xiao D (2000) Single standard calibration for an optical oxygen sensor based on luminescence quenching of a ruthenium complex. Anal Chim Acta 403:57–65
9. Malins C, Fanni S, Glever HG, Vos JG, MacCraith BD (1999) The preparation of a sol–gel glass oxygen sensor incorporating a covalently bound fluorescent dye. Anal Commun 36:3–4
10. Wolfbeis OS, Oehme I, Papkovskaya N, Klimant I (2000) Sol–gel based glucose biosensors employing optical oxygen transducers, and a method for compensating for variable oxygen background. Biosens Bioelectron 15:69–76
11. Dunbar RA, Jordan JD, Bright FV (1996) Development of chemical sensing platforms based on sol−gel-derived thin films: origin of film age vs performance trade-offs. Anal Chem 68:604–610
12. MacCraith BD, McDonagh C (2002) Enhanced fluorescence sensing using sol-gel materials. J Fluoresc 12:333–342
13. Kneas KA, Xu W, Demas JN, DeGraff BA, Zipp AP (1998) Luminescence-based oxygen sensors: $ReL(CO)_3Cl$ and $ReL(CO)_3CN$ complexes on copolymer supports. J Fluoresc 8:295–300
14. Tang Y, Tehan EC, Tao Z, Bright FV (2003) Sol−gel-derived sensor materials that yield linear calibration plots, high sensitivity, and long-term stability. Anal Chem 75:2407–2413
15. Koo YEL, Cao Y, Kopelman R, Koo SM, Brasuel M, Philbert MA (2004) Real-time measurements of dissolved oxygen inside live cells by organically modified silicate fluorescent nanosensors. Anal Chem 76:2498–2505
16. Campostrini R, Ischia M, Carturan G (2002) Sol-gel synthesis and pyrolysis study of oxyfluoride silica gels. J Sol-Gel Sci Technol 23:107–117
17. Atkins GR, Charters RB (2003) Optical properties of highly fluorinated and photosensitive organically-modified silica films for integrated optics. J Sol–Gel SciTechnol 26:919–923
18. Bukowski RM, Ciriminna R, Pagliaro M, Bright FV (2005) High-performance quenchometric oxygen sensors based on fluorinated xerogels doped with $[Ru(dpp)_3]^{2+}$. Anal Chem 77:2670–2672
19. Chu CS, Lo YL (2008) Fiber-optic carbon dioxide sensor based on fluorinated xerogels doped with HPTS. Sens Actuators B: Chem 129:120–125
20. Chu CS, Lo YL (2007) High-performance fiber-optic oxygen sensors based on fluorinated xerogels doped with Pt(II) complexes. Sens Actuators B: Chem 124:376–382
21. Busse S, Scheumann V, Menges B, Mittler S (2002) Sensitivity studies for specific binding reactions using the biotin/streptavidin system by evanescent optical methods. Biosens Bioelectron 17:704–710
22. Ge Z, Brown CW, Sun L, Yang SC (1993) Fiber-optic pH sensor based on evanescent wave absorption spectroscopy. Anal Chem 65:2335–2338
23. Keller BK, DeGrandpre MD, Palmer CP (2007) Waveguiding properties of fiber-optic capillaries for chemical sensing applications. Sens Actuators B: Chem 125:360–371
24. Vogt F, Karlowatz M, Jakusch M, Mizaikoff B (2003) The automated sample preparation system *MixMaster* for investigation of volatile organic compounds with mid-infrared evanescent wave spectroscopy. Analyst 128:397–403
25. Everest MA, Black VM, Haehlen AS, Haveman GA, Kliewer CJ, Neill HA (2006) Hemoglobin adsorption to silica monitored with polarization-dependent evanescent-wave cavity ring-down spectroscopy. J Phys Chem B 110:19461–19468
26. Kumar PS, Lee ST, Vallabhan CPG, Nampoori VPN, Radhakrishnan P (2002) Design and development of an LED based fiber optic evanescent wave sensor for simultaneous detection of chromium and nitrite traces in water. Opt Commun 214:25–30
27. Harrick NJ (1967) Internal reflection spectroscopy. Wiley, New York
28. Yariv A (1989) Quantum electronics, 3rd edn. Wiley, New York, pp 640–649
29. Colthup NB (1964) Introduction to infrared and Raman spectroscopy. Academic, New York
30. Lamber JB, Shurvell HF, Lightner DA, Cooks RG (1998) Organic structural analysis. Prentice Hall, London